Advances in Orbital Angular Momentum Lasers

Andrew Forbes

(Invited Paper)

***Abstract*—As we celebrate 30 years since light's orbital angular momentum (OAM) was connected to its spatial structure, we reflect on the advances made in fundamental science and applications alike. A driving trend in recent times has been the creation of OAM directly from lasers, for potentially tuneable, compact and high-power sources of OAM light. In this tutorial style review we give a summary of the basics of OAM and its creation at the source, pointing to the seminal advances that have been made, the present state-of-the-art, and the open challenges that remain.**

***Index Terms*—Orbital angular momentum, twisted light, vortex beams vector vortex modes structured light, lasers.**

I. Introduction

In THE early part of the previous century light as an electromagnetic wave had become firmly established, while it was already known for some time that light could be polarised. In 1909 Henry Poynting argued that circularly polarised light must carry an angular momentum [1], a spin angular momentum, later reconciled through quantum mechanics and shown to be quantised to $\pm\hbar$ per photon. It was only a few decades later that the mechanical equivalence of photonic angular momentum to mechanical angular momentum was demonstrate, when Richard Beth rotated a physical object (a birefringent waveplate dangling on a thread) with light [2]. Half a century would pass before the orbital component of photonic angular momentum could be linked to light's spatial structure through an azimuthally varying phase, making orbital angular momentum (OAM) light directly associated to conventional Laguerre-Gaussian (LG) laser modes [3]. This opened the path for OAM carrying light to be easily created in optical laboratories, resulting in an explosion of activity in many diverse fields of research.

Scalar OAM beams have been traditionally been created by spiral phase elements [4], [5], mode transformers [3] and q-plates [6], and have found applications in optically rotating objects in optical trapping and tweezing systems [7], [8], metrology of spinning objects [9], phase imaging in a manner that can discern the depth structure [10] and edge enhancement [11], while vortex masks can be used to remove unwanted light in astronomical imaging [12]. Optical communication has seen tremendous advances since early proof-of-principle experiments with OAM [13] to Tera-bits and beyond [14], [15]. Beyond classical studies, quantum states of OAM have been demonstrated [16] and used to access high-dimensional quantum states [17], shown useful for quantum communication [18], [19], [20]. Vectorial OAM beams are easily created in the laboratory using simple glass cones [21], stressed optics [22] and GRIN lenses [23], as well as from spatial light modulators and digital micro-mirror devices [24], [25], non-linear crystals [26], [27], geometric phase elements [6], [28] and metasurfaces [29]. They have been used to drive electric currents [30], [31], imprint the optical patterns into matter [32], enhanced metrological measurements [33], [34], probing single molecules [35] and to encode more information for larger bandwidths [36], [37], [38], [39]. It is beyond the scope of this article to cover this impressive body of work, and instead the reader is referred to many tutorials [40], [41], [42], popular articles [43], [44], [45], reviews [46], [47], [48], [49], [50], [51], [52], [53], [54], [55], [56], [57], [58], [59], [60], [61], [62], [63] and perspectives [64], [65], [66], [67] on the topic.

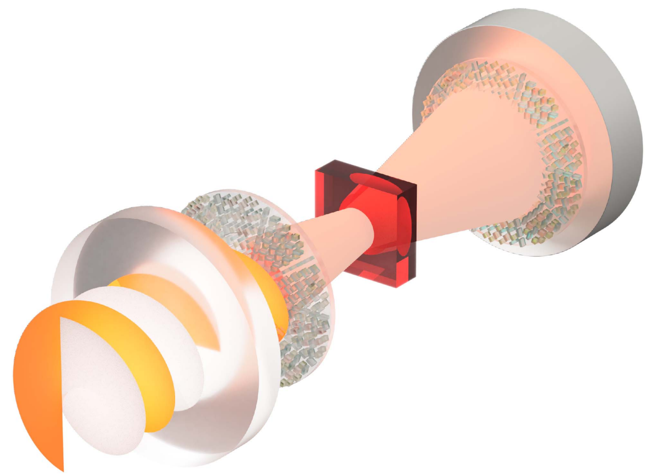

Fig. 1. A structured light laser to produce OAM, using a standard bulk Fabry-Perot cavity as an example. One can enhance mode selection through intra-cavity elements and the mirror shapes, or by shaping the gain (red crystal) through its excitation. The control may be amplitude or phase, but ultimately this only indirectly affects the loss-gain competition of each mode, which directly influences the lasing mode.

One direction that received attention from early on was the creation of OAM directly at the laser source [68], [69], [70], [71], [72], inspired by the initial connection of OAM to the LG laser modes, and illustrated graphically in Fig. 1. And indeed there was early success, although the challenges were also quickly realised. Despite the apparent symmetry of OAM modes, laser

Manuscript received 24 September 2022; revised 31 October 2022; accepted 3 November 2022. Date of publication 8 November 2022; date of current version 3 April 2023.

The author is with the School of Physics, University of the Witwatersrand, Wits 2050, South Africa (e-mail: Andrew.forbes@wits.ac.za).

Color versions of one or more figures in this article are available at https://doi.org/10.1109/JLT.2022.3220509.

Digital Object Identifier 10.1109/JLT.2022.3220509

cavities must often break symmetry in order for Nature to discern the OAM handedness, a clockwise or anticlockwise twist in the azimuthal phase. In this article we briefly review some of the seminal advances, concentrating on recent progress and the open challenges that remain.

II. Back to Basics

To begin with a concrete case, consider the illustrated OAM laser in Fig. 1. To produce OAM from such a laser, the desired OAM mode must have its gain and loss tailored so that it is the first to reach threshold. Such tailoring can be done by intra-cavity elements in bulk lasers, by gain shaping, and by careful attention to the geometry of the laser. In this tutorial style review, we will consider a Laguerre-Gaussian laser mode by way of example, although it should be stressed that any OAM carrying mode would follow a similar argument. A LG mode in cylindrical coordinates can be described by [73]

$$\begin{aligned}\mathrm{LG}_{p\ell}(r,\phi,z) &= \sqrt{\frac{2p!}{\pi w^2(z)(p+|\ell|)!}}L_p^{|\ell|}\left(\frac{2r^2}{w^2(z)}\right)\\ &\times\left(\frac{\sqrt{2}r}{w(z)}\right)^{||\ell|}\exp\left(-\frac{r^2}{w^2(z)}\right)\\ &\times\exp\left(i\eta(z)\right)\exp\left(-\frac{ikr^2}{2R(z)}\right)\exp(i\ell\phi)\end{aligned} \tag{1}$$

where p and ℓ are the radial and azimuthal indices respectively, (r,ϕ) are the transverse coordinates, z is the propagation distance and $L_p^{|\ell|}$ is the generalised Laguerre polynomial. The functional arguments take the form of

$$w(z) = w_0\sqrt{1+\frac{z^2}{z_R^2}}\,,$$

$$R(z) = z\left(1+\frac{z_R^2}{z^2}\right)\,,$$

$$\eta(z) = (2p+|\ell|+1)\arctan\left(\frac{z}{z_R}\right)\,,$$

and

$$z_R = \frac{\pi w_0^2}{\lambda}\,,$$

where w_0 is the Gaussian (fundamental mode) radius at its waist plane ($z=0$) and λ is the wavelength of the light. Such modes are shape invariant during propagation and reduce to the special case of the Gaussian beam when $p=\ell=0$. The OAM modes are identified by the azimuthal phase term $\exp(i\ell\phi)$, where the topological charge, ℓ defines the helicity of the phase, for $\ell\times 2\pi$ phase twists about the azimuth and $\ell\hbar$ of OAM per photon. The twist can be clockwise or anticlockwise for an alphabet that spans $\ell\in[-\infty,\infty]$, and hence the term vortex beams or twisted light to describe OAM light. The radial (r) structure is also OAM dependent through the $\propto r^{|\ell|}$ term in (1) term on line two, while the Laguerre polynomial (in line one) does not contribute unless $p\neq 0$. It is this radially dependent term that gives rise to the on-axis intensity null since it forces the electric field to be zero at $r=0$ while the ℓ in the exponent "flattens" the region near zero to low amplitude. The product of this term and the Gaussian amplitude (also in line two) results in a widening ring of light of radius $r_\ell = w_0\times\sqrt{|\ell|/2}$, which is why such beams are sometimes called donut beams. When this ℓ dependent amplitude is not used in the creation of OAM modes, as is often the case when passing them through just a spiral phase element, then many radial modes are excited (many rings about the desired donut) and little energy in the desired ring [74], [75].

The second moment beam radius and half-angle divergence of these OAM LG modes are in turn given by

$$w_\ell(z) = \sqrt{|\ell|+1}\;w(z) \tag{2}$$

$$\theta_\ell = \sqrt{|\ell|+1}\;\theta_0 \tag{3}$$

where θ_0 is the Gaussian half-angle divergence. This gives rise to the beam quality factor $M^2 = 2p+|\ell|+1$.

A. Vectorial OAM

These scalar OAM modes can be combined with orthogonal polarisation states to form vectorial OAM states, often called vector vortex beams, of the form

$$\mathbf{U} = A_\ell(r,\phi)\left(\exp(i\ell\phi)\hat{R}+\exp(-i\ell\phi+i\gamma)\hat{L}\right), \tag{4}$$

where γ is the intra-modal phase and $\hat{R}$ and $\hat{L}$ are the right-circular and left-circular polarisation states (any orthogonal pair would be fine). These beams combine the spin and orbital components of angular momentum to describe the total angular momentum of light, and can be described geometrically by positions on a High-order Poincaré sphere (HOPS) [76]. In this representation, the poles are circularly polarised OAM scalar modes while the equator returns the cylindrical vector vortex beams [77], known solutions to many optical fibre. Recently it has become commonplace to formulate the above in a quantum language [78], reflecting the fact that such modes of light are non-separable in their two degrees of freedom, so-called classical entanglement [79]. Using Dirac's notation, we can denote a four dimensional space spanned by four scalar OAM modes, $\{|\ell,L\rangle, |-\ell,L\rangle, |-\ell,R\rangle, |-\ell,R\rangle\}$, to form the cylindrical vector vortex modes (our fibre modes) as

$$\begin{aligned}|\mathrm{TM}\rangle &= \frac{1}{\sqrt{2}}(|-\ell,R\rangle+|-\ell,L\rangle),\\ |\mathrm{TE}\rangle &= \frac{-i}{\sqrt{2}}(|-\ell,R\rangle-|-\ell,L\rangle),\\ |\mathrm{HE}\rangle_e &= \frac{1}{\sqrt{2}}(|\ell,L\rangle+|-\ell,R\rangle),\\ |\mathrm{HE}\rangle_o &= \frac{i}{\sqrt{2}}(|\ell,L\rangle-|-\ell,R\rangle).\end{aligned} \tag{5}$$

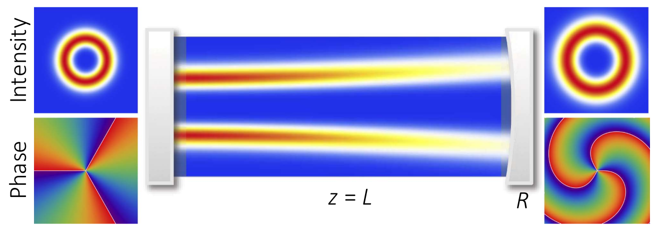

Fig. 2. A cross-section of simple laser cavity with one flat mirror and one curved mirror, overlaid with the propagating LG mode inside. The stable LG beam in such a cavity is shown here for $\ell = 3$ at the two mirrors in intensity and phase.

B. OAM Inside Lasers

How to understand the evolution of such modes inside a laser? For this we unpack the cavity shown in Fig. 1 and illustrate it with the information about how LG modes propagate, shown in Fig. 2. The laser cavity will match the wavefronts of the beam at each mirror. In the example given, this means a flat wavefront at mirror 1 (since $R_1 = \infty$) and a curved wavefront at mirror 2, with radius of curvature $R_2 = R$. To do this one can imagine that the waist size at mirror 1 is altered until the divergence gives the correct radius of curvature after a distance $z = L$ where L is the distance between the two mirrors. The result of this is a second moment beam radius of the OAM mode at the flat mirror of

$$w_\ell = \left(\frac{\lambda}{\pi}\right)\sqrt{L(R-L)(|\ell|+1)}. \tag{6}$$

The resulting beam intensity and phase profiles are shown at each mirror in Fig. 2. To make the laser operate on this mode requires some intervention. It might be in the form of gain around the ring, loss at the centre, or some other mode selection approach. The major challenge is that the radius of curvature, beam size, intensity distribution, Gouy phase and divergence of both helicity OAM states ($\pm|\ell|$) are identical, so that Nature cannot tell them apart, often lasing on both. The result is either an incoherent superposition or a coherent superposition [80], for petal-like modes [81] or donut-like modes [82], the former with OAM and the latter with no OAM. Some examples of OAM modes and their superpositions are shown in Fig. 3.

C. Remarks

There has been some confusion about the nature of light's angular momentum and its link to phase singularities. Optical vortices had been known long before OAM was topical (see Refs. [83], [84] for good historical accounts), but vortices do not equate to OAM [85], and nor is OAM due to an "azimuthal" wavevector - there is no such component to the electric field [86], and further, there is no continuously spirally Poynting vector; rather the Poynting vector makes only modest rotations from the near to the far field [87]. OAM can be both an intrinsic and extrinsic property of light [88], explaining why the OAM can appear to change when measured off-axis. Just as phase vortices do not imply OAM, so too a donut intensity does not imply OAM; such an intensity can arise from an incoherent superposition of

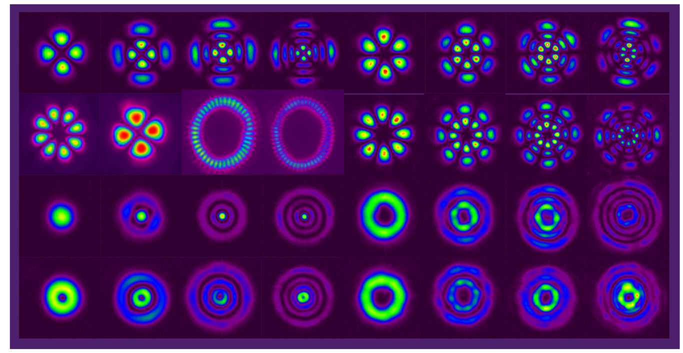

Fig. 3. A myriad of OAM and OAM superpositions produced from a laser with an internal spatial light modulator [82]. The petal-like structures are telltale signs that the two helicities are adding coherently. Not all the donut shaped beams have OAM, while the multiple rings indicate the presence of radial (p) modes.

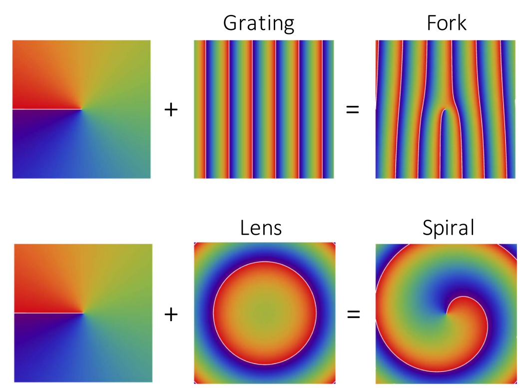

Fig. 4. Azimuthal, forked and spiral phase patterns, shown here for $\ell = 1$. The addition of a tilt or grating leads to a "forked" pattern, whereas the addition of curvature or a lens results in a spiral pattern.

odd and even LG modes with no nett OAM [80]. Similarly, vector vortex beams have polarisation singularities not phase singularities, have a donut shape, and those with symmetric OAM as in (5) have no nett angular momentum.

Finally, the literature is likewise mixed with azimuthal phases, spiral phases and "forked" phases. The origin of each of these is shown in Fig. 4. Each has an azimuthal component, but the spiral phase as an additional radius of curvature (lens) overlaid, while the forked pattern has a tilt (grating) overlaid. This could be deliberate, such as curvature from a laser mirror or tilt from a diffraction grating to alter the direction of the OAM light, but could also be a consequence of the experiment: curvature arises from propagation away from the waist plane, and a tilt can arise of the beam is interfered with another arriving at an angle. A quantitative measure of the OAM content of a beam is to perform a modal decomposition [89], for full reconstruction of not only the total OAM but also the local OAM density [90].

III. Advances With Bulk Lasers

The first reported laser to produce an OAM mode was in a gas CO_2 laser, using intra-cavity cylindrical lenses to control phases and a spiral phase plate so that OAM with a specific helicity could be produced [91]. Since then OAM modes have been produced by amplitude control by spot defects on mirrors [92], pump shaping to form annular gain regions [93] and by changing the geometry of the cavity [94]. The highest reported OAM from a laser is $\ell = 288$, created by an annular ring amplitude mask scribed onto a mirror surface [95]. Lifting the degeneracy of the $\pm\ell$ modes has hindered many approaches but was shown possible by amplitude selection, but required careful tilt control to introduce losses by virtue of the Poynting vector angle of each helicity [96]. Note that traditional phase elements such as spiral phase plates have in general not been successful in OAM lasers because of the problem that the helicity inverts on each bounce off an mirror, so that no repeating mode is formed and the OAM simply ladders up (or down) in value. Recently this has been overcome by combining a digital spiral plate with a defect and a lens, trying to suppress unwanted modes and avoid the sign swapping of the OAM [97]. A general solution to this problem of handedness selectivity was introduced in 2016 by the first OAM laser based on geometric phase, producing scalar OAM and vector superpositions with OAM of up to $\ell = 10$ [99]. The laser used a conventional cavity to control the polarisation state prior to a q-plate, so that OAM could be controlled. Circular polarised states mapped to pure OAM of controlled helicity, while linear polarisation states mapped to vector vortex beams, finally producing all states on the HOPS. Metasurface lasers based on geometric phase reached $\ell = 3$ [100], [101], but it was only after the invention of so-called J-plates [29] that arbitrary OAM coupled to arbitrary polarisation states could be produced. The result was a laser showing up to $\ell = 100$ in scalar OAM beams, and asymetric vectorial superpositions for the first non-zero nett OAM, for instance, lasing on both $\ell = 100$ and $\ell = 10$ simultaneously [102]. All these bulk lasers produced a single spatial mode in OAM. Recently an OAM array laser has been demonstrated [98], as illustrated in Fig. 5. Using a metasurface of 100 (10×10) elements in a degenerate cavity, the individual elements of the array could coherently couple together to form a 100 vortex array as the output. Interestingly, the coupling ensured that defects in the array elements could self-heal and restore the array OAM back to the global value. By adjusting the polarisation inside the cavity, vectorial superpositions could also be created.

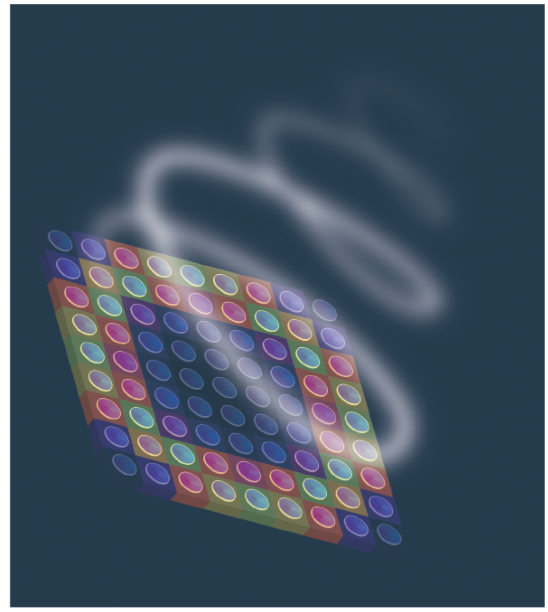

Fig. 5. An artistic impression of a vortex array laser produced by a metasurface made of 10×10 individual elements placed into a Talbot cavity with high modal degeneracy. Coupling between the array elements ensures a coherent combination at the output [98]. Image courtesy of the authors.

IV. Advances With Compact Lasers

Compact solutions for OAM at the source are highly desirable in some applications, for instance, to integrate the source with other on-chip components, or to have small, lightweight solutions for space. In this regard fibre lasers can be compact as compared to traditional bulk solid state lasers. The usual approach to exciting OAM in fibre lasers is to use few or multimode fibre and excite combinations of modes to add to the desired OAM mode. The first scalar OAM modes directly from a fibre laser were reported only recently, first with a stressed large mode area fibre amplifier [103] and later using few mode fibre configurations [104], [105], [106]. Recent advances include high power fibre lasers at femtosecond time frames [107], the use of twisted fibres for twisted light [108]. There is of course a long history of producing vectorial light from optical fibre [71] and OAM in fibre [72], both of course can also be considered advances in OAM fibre lasers. Because this topic has been reviewed only recently [71], [72], we will not delve into further details and refer the reader to these very good reviews for more details.

Integrated solutions date back more than 20 years to the first microchip OAM laser [93] and only much later on-chip OAM lasers [110], integrated vertical-cavity surface-emitting OAM lasers [111] and OAM organic microlasers [112]. Recent advances have concentrated on tuneability in wavelength, OAM and helicity control. One example was the use of time-reversal symmetry breaking in a semiconductor micro-laser to control the helicity of OAM modes. By exciting micro-pillars with a chiral pump, the controlled chirality, left- or right-circularly polarised light, could be used to control the OAM helicity [113]. In a similar vein, spin-orbit interaction was dynamically controlled to alter the emitted OAM state by converting the SAM into OAM, introducing additional tunability with variable topological charges at the same wavelength [109] as shown in Fig. 6. In the latter it was non-hermitian notions that fuelled the advance, while vortex array outputs have been shown viable using unconventional supersymmetric concepts [114]. Even static elements have their benefit, as was shown by the use of monolithic integration of dielectric metasurfaces with VCSELs to enable a range of output modes, including OAM beams with high efficiency [115], with the metasurface approach to controlling emitters recently extended to vortex arrays [116]. An interesting example in tuneable microlasers was the use of an optofluidic microcavity designed laser for vortex beams whose the handedness, topological charges, and lasing wavelengths could be flexibly controlled and even dynamically adjusted [117] as shown in

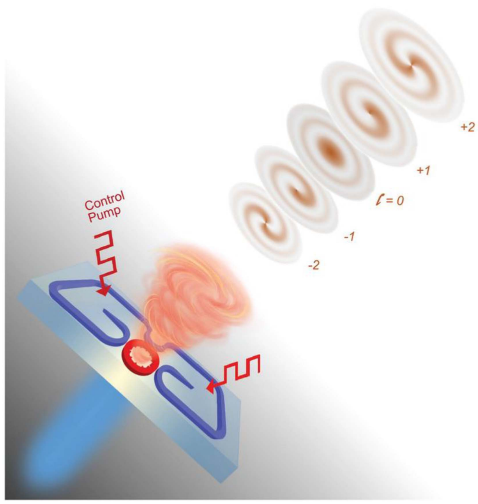

Fig. 6. A microlaser for tuneable OAM. By adjusting the chirality of the pump light, the OAM could be changed dynamically. Adapted from Ref. [109] with permission under CC BY 4.0.

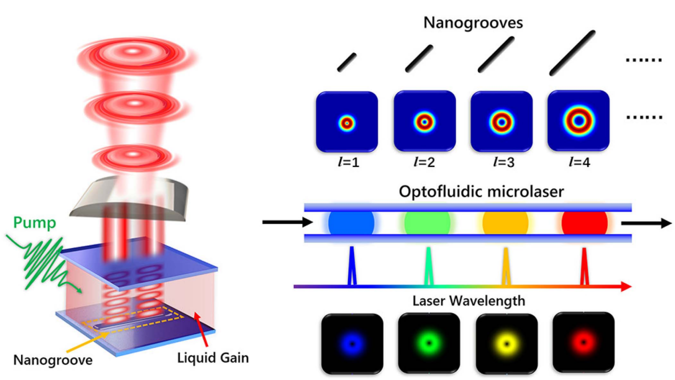

Fig. 7. A microlaser for tuneable OAM and wavelength. Adapted from Ref. [117] with permission under CC BY 4.0.

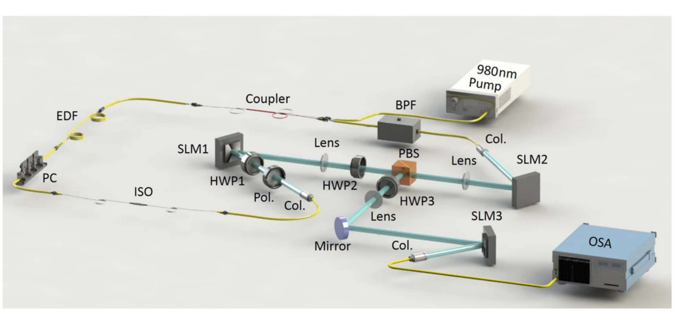

Fig. 8. A hybrid free-space and fibre laser that has reconfigurable OAM states, while operating across a wide wavelength range. Adapted from Ref. [118] with permission under CC BY 4.0.

Fig. 7. The authors fabricated nanogrooves onto the bottom mirror of the laser to force the cavity to lase on Hermite-Gaussian modes, which in turn were converted to OAM modes using a single-cylindrical-lens mode converter. The topological charge was tuned by the length of a nanogroove, the handedness was controlled by the orientation of the cylindrical lens, and the wavelength by the liquid dye inside the optofluidic chamber, serving as the laser gain.

V. Concluding Remarks

The promise of OAM directly from lasers is potentially tuneable, compact and/or high-power sources of OAM light. Although we have made steady progress, there remain some open challenges. High power OAM lasers are highly desirable, with the state of the art reaching up to 1.2 GW of peak power from disk lasers [119], 2 kW from solid-state lasers [120] and 3 kW in average power from fibre lasers [121]. External amplification has been modest, reaching 30 W [122] from solid state OAM lasers. Pushing the power up while increasing modal purity and OAM range remains challenging, as does the structured light toolkit to control and measure such exotic states of light. For instance, vectorial adaptive optics may be needed for the correction of thermally aberrated vectorial modes, a topic still in its infancy [123].

Tuneability in OAM and wavelength remains topical too, reaching up to $\Delta\ell = \pm 15$ by using off-axis pumping (gain shaping with asymmetry) in a solid state laser [124] and $\Delta\lambda \approx 40$ nm and $\Delta\ell = \pm 3$ [125] using a broadband source and a MEMS filter. A good compromise was introduced in a hybrid free-space and fibre system to produce $\Delta\lambda \approx 35$ nm and $\Delta\ell = \pm 10$ [118], illustrated in Fig. 8. The advances are as yet modest, with much work to do in order to have truly broadband operation.

Looking back over 30 years of advances in OAM makes clear the progress made, from unravelling the science to harnessing it for applications. Creating OAM directly at the source is crucial in many arenas, from the compactness required for integrated solutions, to the high power needed for manufacturing. Bulky and low power external solutions are not viable in these areas. Lasers offer the ability to counter the loss, improve the purity, and deliver the OAM on-demand at custom wavelengths and in custom architectures. The emergent field of metasurfaces for OAM creation and control heralds exciting opportunities to blend bulk and compact solutions, as well as to consider non-linear and linear transformations in one package. What this might do for lasers is yet to be fully explored, but surely promises an exciting future. The open challenge is to translate the science into practical laser systems that can be deployed by non-experts in the field. Until we reach this milestone, OAM applications will remain at proof-of-principle stage in scientific laboratories.

References

[1] J. H. Poynting, "The wave motion of a revolving shaft, and a suggestion as to the angular momentum in a beam of circularly polarised light," *Proc. Roy. Soc. London. Ser., A., Containing Papers Math. Phys. Character*, vol. 82, no. 557, pp. 560–567, 1909.

[2] R. A. Beth, "Mechanical detection and measurement of the angular momentum of light," *Phys. Rev.*, vol. 50, pp. 115–125, 1936.

[3] L. Allen, M. W. Beijersbergen, R. J. C. Spreeuw, and J. P. Woerdman, "Orbital angular momentum of light and the transformation of Laguerre-Gaussian laser modes," *Phys. Rev. A*, vol. 45, no. 11, 1992, Art. no. 8185.

[4] N. R. Heckenberg, R. McDuff, C. Smith, and A. G. White, "Generation of optical phase singularities by computer-generated holograms," *Opt. Lett.*, vol. 17, no. 3, pp. 221–223, 1992.

[5] J. Pinnell, V. Rodríguez-Fajardo, and A. Forbes, "Probing the limits of orbital angular momentum generation and detection with spatial light modulators," *J. Opt.*, vol. 23, no. 1, 2020, Art. no. 015602.

[6] L. Marrucci, C. Manzo, and D. Paparo, "Optical spin-to-orbital angular momentum conversion in inhomogeneous anisotropic media," *Phys. Rev. Lett.*, vol. 96, 2006, Art. no. 163905.

[7] H. He, M. E. J. Friese, N. R. Heckenberg, and H. Rubinsztein-Dunlop, "Direct observation of transfer of angular momentum of absorptive particles from a laser beam with a phase singularity," *Phys. Rev. Lett.*, vol. 75, pp. 826–829, 1995.

[8] N. Simpson, K. Dholakia, L. Allen, and M. Padgett, "Mechanical equivalence of spin and orbital angular momentum of light: An optical spanner," *Opt. Lett.*, vol. 22, no. 1, pp. 52–54, 1997.

[9] M. P. Lavery, F. C. Speirits, S. M. Barnett, and M. J. Padgett , "Detection of a spinning object using light's orbital angular momentum," *Science*, vol. 341, no. 6145, pp. 537–540, 2013.

[10] C. Maurer, A. Jesacher, S. Bernet, and M. Ritsch-Marte, "What spatial light modulators can do for optical microscopy," *Laser Photon. Rev.*, vol. 5, no. 1, pp. 81–101, 2011.

[11] B. Jack et al., "Holographic ghost imaging and the violation of a bell inequality," *Phys. Rev. Lett.*, vol. 103, 2009, Art. no. 083602.

[12] J. H. Lee, G. Foo, E. G. Johnson, and G. A. Swartzlander Jr, "Experimental verification of an optical vortex coronagraph," *Phys. Rev. Lett.*, vol. 97, no. 5, 2006, Art. no. 053901.

[13] G. Gibson, M. J. Courtial, and J. Padgett, "Free-space information transfer using light beams carrying orbital angular momentum," *Opt. Exp.*, vol. 12, pp. 5448–5456, 2004.

[14] R. Wang, C. Zhang, Y. Yang, S. Zhu, and X.-C. Yuan, "Focused cylindrical vector beam assisted microscopic pSPR biosensor with an ultra wide dynamic range," *Opt. Lett.*, vol. 37, no. 11, pp. 2091–2093, 2012.

[15] N. Bozinovic et al., "Terabit-scale orbital angular momentum mode division multiplexing in fibers," *Science*, vol. 340, pp. 1545–1548, 2013.

[16] A. Mair, A. Vaziri, G. Weihs, and A. Zeilinger, "Entanglement of the orbital angular momentum states of photons," *Nature*, vol. 412, pp. 313–316, 2001.

[17] A. C. Dada, J. Leach, G. S. Buller, M. J. Padgett, and E. Andersson, "Experimental high-dimensional two-photon entanglement and violations of generalized bell inequalities," *Nature Phys.*, vol. 7, pp. 677–680, 2011.

[18] M. Mafu et al., "Higher-dimensional orbital-angular-momentum-based quantum key distribution with mutually unbiased bases," *Phys. Rev. A*, vol. 88, no. 3, 2013, Art. no. 032305.

[19] A. Sit et al., "High-dimensional intracity quantum cryptography with structured photons," *Optica*, vol. 4, no. 9, pp. 1006–1010, 2017.

[20] D. Cozzolino et al., "Air-core fiber distribution of hybrid vector vortex-polarization entangled states," *Adv. Photon.*, vol. 1, no. 4, 2019, Art. no. 046005.

[21] N. Radwell, R. Hawley, J. Götte, and S. Franke-Arnold, "Achromatic vector vortex beams from a glass cone," *Nature Commun.*, vol. 7, no. 1, pp. 1–6, 2016.

[22] A. M. Beckley, T. G. Brown, and M. A. Alonso, "Full poincaré beams," *Opt. Exp.*, vol. 18, no. 10, pp. 10777–10785, 2010.

[23] C. He et al., "Complex vectorial optics through gradient index lens cascades," *Nature Commun.*, vol. 10, no. 1, pp. 1–8, 2019.

[24] C. Rosales-Guzmán et al., "Polarisation-insensitive generation of complex vector modes from a digital micromirror device," *Sci. Rep.*, vol. 10, no. 1, pp. 1–9, 2020.

[25] J. Chen, Y. Wang, C. Wan, K. Lu, Y. Liu, and Q. Zhan, "Compact vectorial optical field generator based on a 10-megapixel resolution liquid crystal spatial light modulator," *Opt. Commun.*, vol. 495, 2021, Art. no. 127112.

[26] H.-J. Wu et al., "Vectorial nonlinear optics: Type-II second-harmonic generation driven by spin-orbit-coupled fields," *Phys. Rev. A*, vol. 100, no. 5, 2019, Art. no. 053840.

[27] Y. Tang, K. Li, X. Zhang, J. Deng, G. Li, and E. Brasselet, "Harmonic spin–orbit angular momentum cascade in nonlinear optical crystals," *Nature Photon.*, vol. 14, no. 11, pp. 658–662, 2020.

[28] M. G. Nassiri and E. Brasselet, "Multispectral management of the photon orbital angular momentum," *Phys. Rev. Lett.*, vol. 121, no. 21, 2018, Art. no. 213901.

[29] R. C. Devlin, A. Ambrosio, N. A. Rubin, J. B. Mueller, and F. Capasso, "Arbitrary spin-to–orbital angular momentum conversion of light," *Science*, vol. 358, no. 6365, pp. 896–901, 2017.

[30] S. Sederberg, F. Kong, F. Hufnagel, C. Zhang, E. Karimi, and P. B. Corkum, "Vectorized optoelectronic control and metrology in a semiconductor," *Nature Photon.*, vol. 14, no. 11, pp. 680–685, 2020.

[31] Y. Fang et al., "Photoelectronic mapping of the spin–orbit interaction of intense light fields," *Nature Photon.*, vol. 15, no. 2, pp. 115–120, 2021.

[32] M. El Ketara, H. Kobayashi, and E. Brasselet, "Sensitive vectorial optomechanical footprint of light in soft condensed matter," *Nature Photon.*, vol. 15, no. 2, pp. 121–124, 2021.

[33] R. D. Hawley, J. Cork, N. Radwell, and S. Franke-Arnold, "Passive broadband full stokes polarimeter using a Fresnel cone," *Sci. Rep.*, vol. 9, no. 1, pp. 1–8, Feb. 2019.

[34] L. Fang, Z. Wan, A. Forbes, and J. Wang, "Vectorial doppler metrology," *Nature Commun.*, vol. 12, no. 1, pp. 1–10, 2021.

[35] V. Curcio, L. A. Alemán-Castañeda, T. G. Brown, S. Brasselet, and M. A. Alonso, "Birefringent Fourier filtering for single molecule coordinate and height super-resolution imaging with dithering and orientation," *Nature Commun.*, vol. 11, no. 1, pp. 1–13, 2020.

[36] G. Milione et al., "4× 20 Gbit/s mode division multiplexing over free space using vector modes and a q-plate mode (de) multiplexer," *Opt. Lett.*, vol. 40, no. 9, pp. 1980–1983, 2015.

[37] J. Zhang et al., "Fiber vector eigenmode multiplexing based high capacity transmission over 5-km FMF with Kramers-Kronig receiver," *J. Lightw. Technol.*, vol. 39, no. 15, pp. 4932–4938, Aug. 2021.

[38] Z. Zhu et al., "Compensation-free high-dimensional free-space optical communication using turbulence-resilient vector beams," *Nature Commun.*, vol. 12, no. 1, pp. 1–8, 2021.

[39] Y. Zhao and J. Wang, "High-base vector beam encoding/decoding for visible-light communications," *Opt. Lett.*, vol. 40, no. 21, pp. 4843–4846, 2015.

[40] E. Toninelli et al., "Concepts in quantum state tomography and classical implementation with intense light: A tutorial," *Adv. Opt. Photon.*, vol. 11, no. 1, pp. 67–134, 2019.

[41] M. Padgett and L. Allen, "Light with a twist in its tail," *Contemp. Phys.*, vol. 41, no. 5, pp. 275–285, 2000.

[42] C. Rosales-Guzmán and A. Forbes, *How to Shape Light With Spatial Light Modulators*. Bellingham, WA, USA: SPIE Press, 2017.

[43] A. Forbes, "Structured light: Tailored for purpose," *Opt. Photon. News*, vol. 31, no. 6, pp. 24–31, 2020.

[44] S. Franke-Arnold and N. Radwell, "Light served with a twist," *Opt. Photon. News*, vol. 28, no. 6, pp. 28–35, 2017.

[45] N. Davidson, S. Mahler, A. Friesem, and A. Forbes, "Complex-light lasers," *Opt. Photon. News*, vol. 33, no. 5, pp. 26–33, 2022.

[46] S. Franke-Arnold, L. Allen, and M. Padgett, "Advances in optical angular momentum," *Laser Photon. Rev.*, vol. 2, pp. 299–313, 2008.

[47] A. M. Yao and M. J. Padgett, "Orbital angular momentum: Origins, behavior and applications," *Adv. Opt. Photon.*, vol. 3, pp. 161–204, 2011.

[48] M. J. Padgett, "Orbital angular momentum 25 years on," *Opt. Exp.*, vol. 25, no. 10, pp. 11265–11274, 2017.

[49] B. Ndagano, I. Nape, M. A. Cox, C. Rosales-Guzman, and A. Forbes, "Creation and detection of vector vortex modes for classical and quantum communication," *J. Lightw. Technol.*, vol. 36, no. 2, pp. 292–301, 2018.

[50] Y. Shen et al., "Optical vortices 30 years on: OAM manipulation from topological charge to multiple singularities," *Light: Sci. Appl.*, vol. 8, no. 1, pp. 1–29, 2019.

[51] A. Forbes and I. Nape, "Quantum mechanics with patterns of light: Progress in high dimensional and multidimensional entanglement with structured light," *AVS Quantum Sci.*, vol. 1, no. 1, 2019, Art. no. 011701.

[52] A. E. Willner et al., "Recent advances in high-capacity free-space optical and radio-frequency communications using orbital angular momentum multiplexing," *Philos. Trans. Roy. Soc. A: Mathematical, Phys. Eng. Sci.*, vol. 375, 2017, Art. no. 20150439.

[53] A. E. Willner et al., "Optical communications using orbital angular momentum beams," *Adv. Opt. Photon.*, vol. 7, pp. 66–106, Mar. 2015.

[54] A. E. Willner, K. Pang, H. Song, K. Zou, and H. Zhou, "Orbital angular momentum of light for communications," *Appl. Phys. Rev.*, vol. 8, no. 4, 2021, Art. no. 041312.

[55] S. Franke-Arnold, "30 years of orbital angular momentum of light," *Nature Rev. Phys.*, vol. 4, no. 6, pp. 361–361, 2022.

[56] M. Krenn, M. Malik, M. Erhard, and A. Zeilinger, "Orbital angular momentum of photons and the entanglement of Laguerre–Gaussian modes," *Philos. Trans. Roy. Soc. A: Math., Phys. Eng. Sci.*, vol. 375, no. 2087, 2017, Art. no. 20150442.

[57] G. Molina-Terriza, J. P. Torres, and L. Torner, "Twisted photons," *Nature Phys.*, vol. 3, no. 5, pp. 305–310, 2007.

[58] X. Wang, Z. Nie, Y. Liang, J. Wang, T. Li, and B. Jia, "Recent advances on optical vortex generation," *Nanophotonics*, vol. 7, no. 9, pp. 1533–1556, 2018.

[59] J. Wang, F. Castellucci, and S. Franke-Arnold, “Vectorial light–matter interaction: Exploring spatially structured complex light fields,” *AVS Quantum Sci.*, vol. 2, no. 3, 2020, Art. no. 031702.

[60] E. Otte, C. Alpmann, and C. Denz, “Polarization singularity explosions in tailored light fields,” *Laser Photon. Rev.*, vol. 12, no. 6, 2018, Art. no. 1700200.

[61] C. Rosales-Guzmän, B. Ndagano, and A. Forbes, “A review of complex vector light fields and their applications,” *J. Opt.*, vol. 20, no. 12, 2018, Art. no. 123001.

[62] A. Forbes, A. Dudley, and M. McLaren, “Creation and detection of optical modes with spatial light modulators,” *Adv. Opt. Photon.*, vol. 8, pp. 200–227, 2016.

[63] A. Rubano, F. Cardano, B. Piccirillo, and L. Marrucci, “Q-plate technology: A progress review,” *J. Opt. Soc. Amer. B*, vol. 36, no. 5, pp. D70–D87, 2019.

[64] C. He, Y. Shen, and A. Forbes, “Towards higher-dimensional structured light,” *Light: Sci. Appl.*, vol. 11, no. 1, pp. 1–17, 2022.

[65] M. Erhard, R. Fickler, M. Krenn, and A. Zeilinger, “Twisted photons: New quantum perspectives in high dimensions,” *Light: Sci. Appl.*, vol. 7, pp. 17111–17146, 2018.

[66] H. Yang, Z. Xie, H. He, Q. Zhang, and X. Yuan, “A perspective on twisted light from on-chip devices,” *APL Photon.*, vol. 6, no. 11, 2021, Art. no. 110901.

[67] A. Forbes, S. Ramachandran, and Q. Zhan, “Photonic angular momentum: Progress and perspectives,” *Nanophotonics*, vol. 11, no. 4, pp. 625–631, 2022.

[68] A. Forbes, “Structured light from lasers,” *Laser Photon. Rev.*, vol. 13, no. 11, 2019, Art. no. 1900140.

[69] A. Forbes, “Controlling light’s helicity at the source: Orbital angular momentum states from lasers,” *Philos. Trans. Roy. Soc., A* vol. 375, no. 2087, 2017, Art. no. 20150436.

[70] T. Omatsu, K. Miyamoto, and A. J. Lee, “Wavelength-versatile optical vortex lasers,” *J. Opt.*, vol. 19, no. 12, 2017, Art. no. 123002.

[71] D. Mao et al., “Generation of polarization and phase singular beams in fibers and fiber lasers,” *Adv. Photon.*, vol. 3, no. 1, 2021, Art. no. 014002.

[72] Y. Lian, Y. Yu, S. Han, N. Luan, Y. Wang, and Z. Lu, “OAM beams generation technology in optical fiber: A review,” *IEEE Sensors J.*, vol. 22, no. 5, pp. 3828–3843, Mar. 2022.

[73] A. Forbes, *Laser Beam Propagation: Generation and Propagation of Customized Light*. Boca Raton, FL, USA: CRC, 2014.

[74] B. Sephton, A. Dudley, and A. Forbes, “Revealing the radial modes in vortex beams,” *Appl. Opt.*, vol. 55, no. 28, pp. 7830–7835, 2016.

[75] E. Karimi, G. Zito, B. Piccirillo, L. Marrucci, and E. Santamato, “Hypergeometric-Gaussian modes,” *Opt. Lett.*, vol. 32, no. 21, pp. 3053–3055, 2007.

[76] G. Milione, H. I. Sztul, D. a. Nolan, and R. R. Alfano, “Higher-order poincaré sphere, stokes parameters, and the angular momentum of light,” *Phys. Rev. Lett.*, vol. 107, 2011, Art. no. 053601.

[77] Q. Zhan, “Cylindrical vector beams: From mathematical concepts to applications,” *Adv. Opt. Photon.*, vol. 1, pp. 1–57, 2009.

[78] T. Konrad and A. Forbes, “Quantum mechanics and classical light,” *Contemporary Phys.*, vol. 60, pp. 1–22, 2019.

[79] A. Forbes, A. Aiello, and B. Ndagano, “Classically entangled light,” *Prog. Opt.*, vol. 64, p. 99, 2019.

[80] I. A. Litvin, S. Ngcobo, D. Naidoo, K. Ait-Ameur, and A. Forbes, “Doughnut laser beam as an incoherent superposition of two petal beams,” *Opt. Lett.*, vol. 39, no. 3, pp. 704–707, 2014.

[81] D. Naidoo, K. Aït-Ameur, M. Brunel, and A. Forbes, “Intra-cavity generation of superpositions of Laguerre–Gaussian beams,” *Appl. Phys. B*, vol. 106, no. 3, pp. 683–690, 2012.

[82] S. Ngcobo, I. Litvin, L. Burger, and A. Forbes, “A digital laser for on-demand laser modes,” *Nature Commun.*, vol. 4, no. 1, pp. 1–6, 2013.

[83] M. Soskin and M. Vasnetsov, “Singular optics,” *Prog. Opt.*, vol. 42, no. 4, pp. 219–276, 2001.

[84] M. R. Dennis, K. O’Holleran, and M. J. Padgett, “Singular optics: Optical vortices and polarization singularities,” in *Prog. Opt*, 2009, vol. 53, pp. 293–363.

[85] M. V. Berry and W. Liu, “No general relation between phase vortices and orbital angular momentum,” *J. Phys. A: Math. Theor.*, vol. 55, no. 37, 2022, Art. no. 374001.

[86] F. C. Speirits and S. M. Barnett, “Do waves carrying orbital angular momentum possess azimuthal linear momentum?,” *Phys. Rev. Lett.*, vol. 111, no. 10, 2013, Art. no. 103602.

[87] M. Padgett and L. Allen, “The poynting vector in Laguerre-Gaussian laser modes,” *Opt. Commun.*, vol. 121, no. 1-3, pp. 36–40, 1995.

[88] A. O’neil, I. MacVicar, L. Allen, and M. Padgett, “Intrinsic and extrinsic nature of the orbital angular momentum of a light beam,” *Phys. Rev. Lett.*, vol. 88, no. 5, 2002, Art. no. 053601.

[89] J. Pinnell, I. Nape, B. Sephton, M. A. Cox, V. Rodríguez-Fajardo, and A. Forbes, “Modal analysis of structured light with spatial light modulators: A practical tutorial,” *JOSA A*, vol. 37, no. 11, pp. C146–C160, 2020.

[90] C. Schulze, A. Dudley, D. Flamm, M. Duparré, and A. Forbes, “Measurement of the orbital angular momentum density of light by modal decomposition,” *New J. Phys.*, vol. 15, Jul. 2013, Art. no. 073025.

[91] R. Oron, N. Davidson, A. A. Friesem, and E. Hasman, “Efficient formation of pure helical laser beams,” *Opt. Commun.*, vol. 182, no. 1, pp. 205–208, 2000.

[92] A. Ito, Y. Kozawa, and S. Sato, “Generation of hollow scalar and vector beams using a spot-defect mirror,” *J. Opt. Soc. Amer. A*, vol. 27, no. 9, pp. 2072–2077, 2010.

[93] Y. Chen and Y. Lan, “Transverse pattern formation of optical vortices in a microchip laser with a large fresnel number,” *Phys. Rev. A*, vol. 65, no. 1, 2001, Art. no. 013802.

[94] M. Okida, T. Omatsu, M. Itoh, and T. Yatagai, “Direct generation of high power Laguerre-Gaussian output from a diode-pumped nd: YVO 4 1.3-μm bounce laser,” *Opt. Exp.*, vol. 15, no. 12, pp. 7616–7622, 2007.

[95] Z. Qiao et al., “Generating high-charge optical vortices directly from laser up to 288th order,” *Laser Photon. Rev.*, vol. 12, no. 8, 2018, Art. no. 1800019.

[96] D. Lin, J. Daniel, and W. Clarkson, “Controlling the handedness of directly excited Laguerre–Gaussian modes in a solid-state laser,” *Opt. Lett.*, vol. 39, no. 13, pp. 3903–3906, 2014.

[97] Y.-Y. Lin and Y.-W. Li, “Spiral-phase-defect resonator and its application in vortex laser of controllable topological charges,” *IEEE Photon. J.*, vol. 14, no. 5, pp. 1–7, Oct. 2022.

[98] M. Piccardo, M. de Oliveira, A. Toma, V. Aglieri, A. Forbes, and A. Ambrosio, “Vortex laser arrays with topological charge control and self-healing of defects,” *Nature Photon.*, vol. 16, no. 5, pp. 359–365, 2022.

[99] D. Naidoo et al., “Controlled generation of higher-order Poincar sphere beams from a laser,” *Nature Photon.*, vol. 10, no. 5, p. 327–332, 2016.

[100] E. Maguid et al., “Topologically controlled intracavity laser modes based on pancharatnam-berry phase,” *ACS Photon.*, vol. 5, no. 5, pp. 1817–1821, 2018.

[101] R. Chriki et al., “Spin-controlled twisted laser beams: Intra-cavity multi-tasking geometric phase metasurfaces,” *Opt. Exp.*, vol. 26, no. 2, pp. 905–916, 2018.

[102] H. Sroor et al., “High-purity orbital angular momentum states from a visible metasurface laser,” *Nature Photon.*, vol. 14, no. 8, pp. 498–503, 2020.

[103] Y. Tanaka, M. Okida, K. Miyamoto, and T. Omatsu, “High power picosecond vortex laser based on a large-mode-area fiber amplifier,” *Opt. Exp.*, vol. 17, no. 16, pp. 14362–14366, 2009.

[104] D. Lin and W. A. Clarkson, “Polarization-dependent transverse mode selection in an Yb-doped fiber laser,” *Opt. Lett.*, vol. 40, no. 4, pp. 498–501, 2015.

[105] T. Wang et al., “Generation of femtosecond optical vortex beams in all-fiber mode-locked fiber laser using mode selective coupler,” *J. Lightw. Technol.*, vol. 35, no. 11, pp. 2161–2166, 2017.

[106] S. Yao, G. Ren, Y. Shen, Y. Jiang, B. Zhu, and S. Jian, “Tunable orbital angular momentum generation using all-fiber fused coupler,” *IEEE Photon. Technol. Lett.*, vol. 30, no. 1, pp. 99–102, Jan. 2018.

[107] D. Lin, Y. Feng, Z. Ren, and D. J. Richardson, “The generation of femtosecond optical vortex beams with megawatt powers directly from a fiber based Mamyshev oscillator,” *Nanophotonics*, vol. 11, no. 4, pp. 847–854, 2022.

[108] M. Bernas, K. Zolnacz, M. Napiorkowski, G. Statkiewicz-Barabach, and W. Urbanczyk, “Conversion of lp 11 modes to vortex modes in a gradually twisted highly birefringent optical fiber,” *Opt. Lett.*, vol. 46, no. 18, pp. 4446–4449, 2021.

[109] Z. Zhang et al., “Tunable topological charge vortex microlaser,” *Science*, vol. 368, no. 6492, pp. 760–763, 2020.

[110] X. Cai et al., “Integrated compact optical vortex beam emitters,” *Science*, vol. 338, no. 6105, pp. 363–366, 2012.

[111] H. Li et al., “Orbital angular momentum vertical-cavity surface-emitting lasers,” *Optica*, vol. 2, no. 6, pp. 547–552, 2015.

[112] H. Qian, B. Markman, and N. Giebink, “Vector vortex beam emission from organic semiconductor microlasers,” *Appl. Phys. Lett.*, vol. 103, no. 16, 2013, Art. no. 161110.

[113] N. C. Zambon et al., "Optically controlling the emission chirality of microlasers," *Nature Photon.*, vol. 13, no. 4, pp. 283–288, 2019.

[114] X. Qiao et al., "Higher-dimensional supersymmetric microlaser arrays," *Science*, vol. 372, no. 6540, pp. 403–408, 2021.

[115] Y.-Y. Xie et al., "Metasurface-integrated vertical cavity surface-emitting lasers for programmable directional lasing emissions," *Nature Nanotechnol.*, vol. 15, no. 2, pp. 125–130, 2020.

[116] H. Zhang et al., "All-dielectric metasurface-enabled multiple vortex emissions," *Adv. Mater.*, vol. 34, no. 14, 2022, Art. no. 2109255.

[117] Z. Qiao et al., "Tunable optical vortex from a nanogroove-structured optofluidic microlaser," *Nano Lett.*, vol. 22, no. 3, pp. 1425–1432, 2021.

[118] N. Zhou, J. Liu, and J. Wang, "Reconfigurable and tunable twisted light laser," *Sci. Rep.*, vol. 8, no. 1, 2018, Art. no. 11394.

[119] J.-P. Negel et al., "Thin-disk multipass amplifier for fs pulses delivering 400 W of average and 2.0 GW of peak power for linear polarization as well as 235 W and 1.2 GW for radial polarization," *Appl. Phys. B*, vol. 123, no. 5, 2017, Art. no. 156.

[120] I. Moshe, S. Jackel, A. Meir, Y. Lumer, and E. Leibush, "2kW, $M^2 <$ 10 radially polarized beams from aberration-compensated rod-based Nd: YAG lasers," *Opt. Lett.*, vol. 32, no. 1, pp. 47–49, 2007.

[121] M. A. Ahmed, J. Schulz, A. Voss, O. Parriaux, J.-C. Pommier, and T. Graf, "Radially polarized 3kw beam from a CO_2 laser with an intracavity resonant grating mirror," *Opt. Lett.*, vol. 32, no. 13, pp. 1824–1826, 2007.

[122] J. Geberbauer, W. Kerridge-Johns, and M. Damzen, "$>$ 30 W vortex LG_{01} or HG_{10} laser using a mode transforming output coupler," *Opt. Exp.*, vol. 29, no. 18, pp. 29082–29094, 2021.

[123] C. He, J. Antonello, and M. J. Booth, "Vectorial adaptive optics," 2021, *arXiv:2110.02606*.

[124] Y. Shen, Y. Meng, X. Fu, and M. Gong, "Wavelength-tunable Hermite–Gaussian modes and an orbital-angular-momentum-tunable vortex beam in a dual-off-axis pumped Yb: CALGO laser," *Opt. Lett.*, vol. 43, no. 2, pp. 291–294, 2018.

[125] V. S. Lyubopytov et al., "Simultaneous wavelength and orbital angular momentum demultiplexing using tunable MEMS-based Fabry-Perot filter," *Opt. Exp.*, vol. 25, no. 9, pp. 9634–9646, 2017.